Analysis and Optimization of Elliptic Ridged Waveguide with FDFD Technique and PSO Algorithm

Alessandro Fanti, Marco Simone, and Luisa Deias

Department of Electrical and Electronic Engineering
University of Cagliari, 09123, Piazza d'Armi, Cagliari, Italy
{alessandro.fanti, marco.simone, luisa.deias }@diee.unica.it

Abstract ─ A new design technique for elliptic ridged and sectoral waveguides is presented. The PSO technique has been employed, using FDFD to compute the propagation data of the guide. Conflicting requirements of wide bandwidth and high power handling capability are taken both into account with a suitable objective function.

Index Terms ─ Cutoff frequency, elliptical ridged waveguide analysis, finite difference frequency domain, microwave components, microwave filters, optimization, PSO, ridged waveguides, waveguide modes.

I. INTRODUCTION

In many applications, microwave propagation structures with high power handling capabilities and low-losses are required. The most effective structures which satisfy these requests are metallic hollow waveguides (WG). The modal structure [1] of WG propagation implies that WGs can be used only as long as single mode propagation takes place. Moreover, the propagation of each mode is high-pass and dispersive. Therefore, the useful bandwidth of a given WG is relatively narrow. The most popular approach to increase significantly the bandwidth, retaining all the useful WG properties, is the use of ridged waveguides R-WG [2].

First studies on R-WGs were made by Cohn [3], who showed how rectangular ridge waveguides have a lower cutoff frequency and a greater bandwidth compared to a standard rectangular waveguide with the same dimensions. Then Hopfer [4] analysed the microwave properties of single and double ridge waveguide, such as cut-off frequency, bandwidth, attenuation and power handling: in particular he showed that a ridge structure provides a larger bandwidth but, on the other hand, it has a reduced power handling capability. Transverse resonance technique [5] has been the first approach of analysis of rectangular R-WG, [2] despite its reduced accuracy. Application of ridged circular waveguides, ridged elliptic waveguides (REW) and sectoral elliptic waveguides (SEW) [6] can be found in many components like filters, matching networks, orthomode transducers, polarizers and circulators that are widely used in satellite and terrestrial communication systems [7]-[11]. Low-cost design, small size, and optimum performance of these components are essential to satisfy today's stringent payload requirements.

An analytical, closed form solution exists also for elliptic waveguides, and has been found by Chu [12] since the 30's. Unfortunately, the field distribution is described by the Mathieu functions [13], whose numerical evaluation is very cumbersome. The best approach seems the expansion of those functions in a series of (more tractable) Bessel functions [14]. In [15], the cutoff wavelengths have been computed efficiently applying by the method of fundamental solutions. In [16], using Mathieu functions and their addition theorem, was presented the general exact solution for evaluation the cutoff frequency in eccentric elliptical waveguides.

Aim of this work is to devise a FDFD [17]-[20] approach for SEW [21] and REW homogeneous elliptic waveguides, tailored to the structure, but as simple as the standard one in the formulation. Use of a suitable elliptical grid (which perfectly fits the waveguide boundary) allows to evaluate the SEW and REW modes with the required accuracy using order of magnitude less sampling points than the standard approach of FDFD [22], namely the use of a rectangular grid with a staircase approximation of the boundary. In addition a REW configuration have been effectively optimized through a synergic use of PSO and the FDFD, aiming at the best trade trade-off of the different requirements of bandwidth and power handling.

II. DESCRIPTION OF FDFD TECNIQUE

The TE and TM modes of waveguide can be calculated [1] by solving the eigenvalue equation $\nabla_t^2\phi = -k_t^2\phi$, with the boundary conditions (BC) $\partial\phi/\partial n = 0$ for TE modes and $\phi = 0$ for TM modes. In the eigenvalue equation ϕ is a scalar potential and k_t is

Submitted On: February 27, 2015
Accepted On: Novenber 8, 2015

the "transverse eigenvalue", from which the propagation constant and the characteristic impedance can be obtained. Apart some canonical geometries, this eigenvalue problem must be solved numerically. Probably, the most effective approach is FDFD [23], i.e., the direct discretization of the problem on a suitable grid. Such a technique has been shown to be well suitable to ridge waveguide through proper approximations of the equation and the boundary conditions (BC). A rectangular lattice of sampling points is a very accurate grid for rectangular and staircase ridges [23], whereas it reduces a curvilinear geometry to a staircase approximate structure. Since the analysis presented in this paper is focused on elliptic boundaries, a set of sampling points in elliptic coordinate has been considered (Fig. 1).

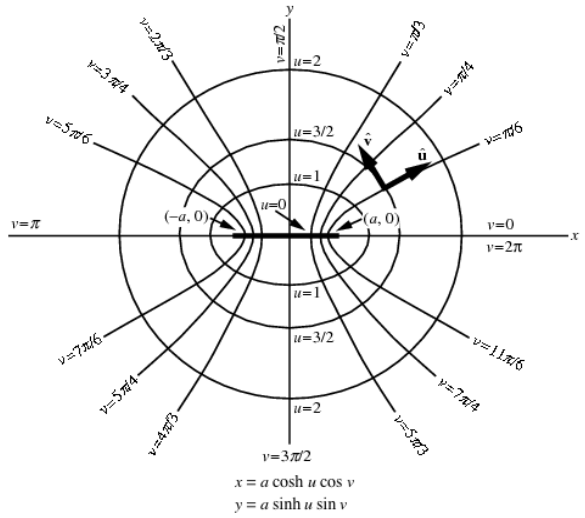

Fig. 1. Geometry of the elliptic coordinates [24].

Let's define Δu, Δv the spacing steps, and $\phi_{pq} = \phi(p\Delta u, q\Delta v)$. The elliptical grid is characterized by a number of points n_u and n_v respectively along the axes u and v. The Helmholtz equation takes the form:

$$\frac{1}{a^2\left(\sinh^2 p\Delta u + \sin^2 q\Delta v\right)} \cdot \left[\frac{\partial^2\phi}{\partial u^2} + \frac{\partial^2\phi}{\partial v^2}\right]_{pq} = -k_t^2\phi_{pq}. \quad (1)$$

For each internal point P (see Fig. 2) is simpler to discretize the term in brackets (1) using a fourth-order Taylor expansion,

$$\phi_B = \phi_P + \left.\frac{\partial\phi}{\partial u}\right|_P \cdot(-\Delta u) + \frac{1}{2}\left.\frac{\partial^2\phi}{\partial u^2}\right|_P \cdot(-\Delta u)^2 + \\ + \frac{1}{6}\left.\frac{\partial^3\phi}{\partial u^3}\right|_P \cdot(-\Delta u)^3 + \frac{1}{24}\left.\frac{\partial^4\phi}{\partial u^4}\right|_P \cdot(-\Delta u)^4 \quad , \quad (2)$$

$$\phi_N = \phi_P + \left.\frac{\partial\phi}{\partial u}\right|_P \cdot(-2\Delta u) + \frac{1}{2}\left.\frac{\partial^2\phi}{\partial u^2}\right|_P \cdot(-2\Delta u)^2 + \\ + \frac{1}{6}\left.\frac{\partial^3\phi}{\partial u^3}\right|_P \cdot(-2\Delta u)^3 + \frac{1}{24}\left.\frac{\partial^4\phi}{\partial u^4}\right|_P \cdot(-2\Delta u)^4 \quad , \quad (3)$$

$$\phi_D = \phi_P + \left.\frac{\partial\phi}{\partial u}\right|_P \cdot(\Delta u) + \frac{1}{2}\left.\frac{\partial^2\phi}{\partial u^2}\right|_P \cdot(\Delta u)^2 + \\ + \frac{1}{6}\left.\frac{\partial^3\phi}{\partial u^3}\right|_P \cdot(\Delta u)^3 + \frac{1}{24}\left.\frac{\partial^4\phi}{\partial u^4}\right|_P \cdot(\Delta u)^4 \quad , \quad (4)$$

$$\phi_Q = \phi_P + \left.\frac{\partial\phi}{\partial u}\right|_P \cdot(2\Delta u) + \frac{1}{2}\left.\frac{\partial^2\phi}{\partial u^2}\right|_P \cdot(2\Delta u)^2 + \\ + \frac{1}{6}\left.\frac{\partial^3\phi}{\partial u^3}\right|_P \cdot(2\Delta u)^3 + \frac{1}{24}\left.\frac{\partial^4\phi}{\partial u^4}\right|_P \cdot(2\Delta u)^4 \quad , \quad (5)$$

leading to:

$$\left.\frac{\partial^2\phi}{\partial u^2}\right|_P = \frac{1}{12\Delta u^2}\cdot\left(16\phi_B + 16\phi_D - \phi_N - \phi_Q - 30\phi_P\right). \quad (6)$$

By repeating the same for the v direction:

$$\left.\frac{\partial^2\phi}{\partial v^2}\right|_P = \frac{1}{\Delta v^2}\cdot\left(16\phi_H + 16\phi_G - \phi_A - \phi_C - 30\phi_P\right), \quad (7)$$

an approximation of the term in square brackets is obtained:

$$\left[\frac{\partial^2\phi}{\partial u^2} + \frac{\partial^2\phi}{\partial v^2}\right] = \\ \frac{16}{12\Delta v^2}\cdot\phi_H + \frac{16}{12\Delta v^2}\cdot\phi_G - \frac{1}{12\Delta v^2}\cdot\phi_A - \frac{1}{12\Delta v^2}\cdot\phi_C \\ \frac{16}{12\Delta u^2}\cdot\phi_B + \frac{16}{12\Delta u^2}\cdot\phi_D - \frac{1}{12\Delta u^2}\cdot\phi_N - \frac{1}{12\Delta u^2}\cdot\phi_Q \\ -\frac{30}{12}\left(\frac{1}{\Delta u^2} + \frac{1}{\Delta v^2}\right)\cdot\phi_P \quad , \quad (8)$$

which provides an approximation of the Helmholtz equation suitable to the FDFD's application.

Due to geometric singularities, Equation (8) is not applicable in the two foci, in the segment of points between them and in the external points.

For a generic point P in the segment joining the two foci, it is possible to integrate $\nabla_t^2\phi = -k_t^2\phi$:

$$\int \nabla_t^2\phi dS = -k_t^2\int \phi dS\theta, \quad (9)$$

and apply the Gauss theorem:

$$\int_{\Gamma_F} \frac{\partial\phi}{\partial n}\cdot dl = -k_t^2\int_{S_F}\phi dS, \quad (10)$$

wherein S_F is the cell surface, and Γ_F is the cell boundary.

The grid presents two types of boundary points, the

radial ones (Fig. 3 (a)) and the angular ones (Fig. 3 (b)).

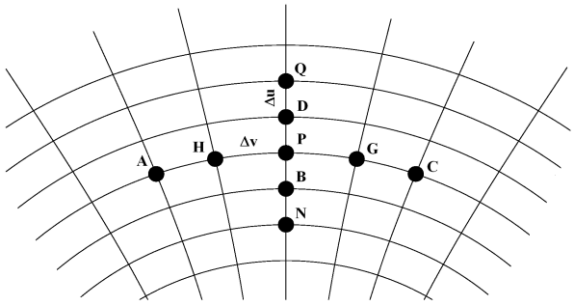

Fig. 2. Internal point of the elliptic coordinates grid TE and TM.

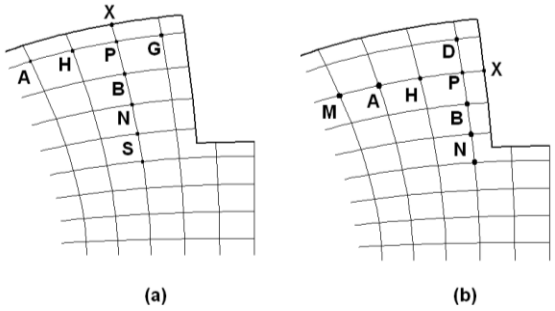

Fig. 3. (a) Radial boundary point P, and (b) angular boundary point P.

Both the boundary points request the same enforcement of the TE boundary conditions, so only the radial one will be considered. The point X in Fig. 3 (a) is not a discretization point, so the application of the Taylor expansion would require the computation of $\phi(u)$ outside the sampling region. Therefore a different approach has been devised using either ϕ_X to enforce the boundary condition $\frac{\partial\phi}{\partial n}=0$.

By considering an "edge" sampling point P (Fig. 3 (a)), the second derivative in u direction can be written as follows:

$$\left.\frac{\partial^2\phi}{\partial u^2}\right|_P \cong \sum_{i=B,N,S} F_i\left(\phi_i-\phi_P\right)= \\ =\left[T_1\left.\frac{\partial\phi}{\partial u}\right|_P+T_2\left.\frac{\partial^2\phi}{\partial u^2}\right|_P+T_3\left.\frac{\partial^3\phi}{\partial u^3}\right|_P+T_4\left.\frac{\partial^4\phi}{\partial u^4}\right|_P\right], \quad (11)$$

where:

$$T_1=\sum_{i=B,N,S}F_i\cdot\Delta u_i,\ T_2=\sum_{i=B,N,S}A_i\cdot\Delta u_i^2,\\ T_3=\sum_{i=B,N,S}F_i\cdot\Delta u_i^3,\ T_4=\sum_{i=B,N,S}F_i\cdot\Delta u_i^4,$$

are linear combination of the unknown coefficient F_i, and B,N,S is the points used in the expression of coefficient B.

Now can be expanded $\partial\phi/\partial u=0$ using a Taylor series:

$$\left.\frac{\partial\phi}{\partial u}\right|_X \simeq \left.\frac{\partial\phi}{\partial u}\right|_P+\left.\frac{\partial^2\phi}{\partial u^2}\right|_P\cdot\left(\frac{\Delta u}{2}\right)+ \\ +\frac{1}{2}\left.\frac{\partial^3\phi}{\partial u^3}\right|_P\cdot\left(\frac{\Delta u}{2}\right)^2+\frac{1}{6}\left.\frac{\partial^4\phi}{\partial u^4}\right|_P\cdot\left(\frac{\Delta u}{2}\right)^3=0, \quad (12)$$

which can be solved for $\left.\frac{\partial\phi}{\partial u}\right|_P$. Its expression can be used to replace the first term in the right hand side of Equation (11):

$$\left(T_2-T_1\frac{\Delta u}{2}\right)\cdot\left.\frac{\partial^2\phi}{\partial u^2}\right|_P+\left(T_3-T_1\frac{\Delta u^2}{8}\right)\cdot\left.\frac{\partial^3\phi}{\partial u^3}\right|_P+ \\ +\left(T_4-T_1\frac{\Delta u^3}{48}\right)\left.\frac{\partial^4\phi}{\partial u^4}\right|_P. \quad (13)$$

Equation (13) is an approximation of $\frac{\partial^2\phi}{\partial u^2}$ if:

$$T_2-T_1\frac{\Delta u}{2}=1,\ T_3-T_1\frac{\Delta u^2}{8}=0,\ T_4-T_1\frac{\Delta u^3}{48}=0,$$

and coefficients F_i are given by the solution of the linear system (13), so (6) is replaced, in this case by:

$$\left.\frac{\partial^2\phi}{\partial u^2}\right|_P=\frac{1}{24\Delta u^2}\cdot\left(21\phi_B+3\phi_N-\phi_S-23\phi_P\right), \quad (14)$$

and the Equation (8) became:

$$\frac{21}{24\Delta u^2}\phi_B+\frac{3}{24\Delta u^2}\phi_N-\frac{1}{24\Delta u^2}\phi_S+ \\ +\frac{\phi_H}{\Delta v^2}+\frac{\phi_G}{\Delta v^2}-\left(\frac{23}{24\Delta u^2}+\frac{2}{\Delta v^2}\right)\phi_P\cong-k_t^2\phi_P^2, \quad (15)$$

A significant advantage of the present approach is that TM modes can be computed on the same TE grid, at variance of the standard approach [22], which calls for two different sets of sampling points, to cope with the different BC (2). To get the TM modes on the same grid, as TE, only the BC needs to be changed to, which becomes $\phi_X=0$ (see Fig. 3 (a)). This BC can be enforced by expressing the potential in X has been approximated through Taylor:

$$\phi_X=\phi_P+\left.\frac{\partial\phi}{\partial u}\right|_P\cdot\left(\frac{\Delta u}{2}\right)+\frac{1}{2}\left.\frac{\partial^2\phi}{\partial u^2}\right|_P\cdot\left(\frac{\Delta u}{2}\right)^2+ \\ +\frac{1}{6}\left.\frac{\partial^3\phi}{\partial u^3}\right|_P\cdot\left(\frac{\Delta u}{2}\right)^3+\frac{1}{24}\left.\frac{\partial^4\phi}{\partial u^4}\right|_P\cdot\left(\frac{\Delta u}{2}\right)^4, \quad (16)$$

and set $\phi_X=0$. The second derivative in P (17) is obtained by adding (11) and (16), and solving the linear system (13):

$$\left.\frac{\partial^2\phi}{\partial u^2}\right|_P = \frac{7}{3\Delta u^2}\phi_B - \frac{2}{5\Delta u^2}\phi_N + \frac{1}{21\Delta u^2}\phi_S - \frac{16}{3\Delta u^2}\phi_P \,. \quad (17)$$

The final expression is obtained from the combination of (7) and (17) into (8):

$$\begin{aligned} &\frac{7}{3\Delta u^2}\phi_B - \frac{2}{5\Delta u^2}\phi_N + \frac{1}{21\Delta u^2}\phi_S + \\ &\frac{1}{3\Delta v^2}\phi_G + \frac{5}{3\Delta v^2}\phi_H - \frac{2}{15\Delta v^2}\phi_A + \\ &-\left(\frac{4}{\Delta v^2} + \frac{16}{3\Delta u^2}\right)\phi_P \cong -k_t^2\phi_P^2 \end{aligned} \quad . \quad (18)$$

Of course all other points can be dealt with in the same way as for TE modes.

III. DESCRIPTION OF PSO

PSO is an iterative algorithm designed to find out the solution of optimization problems, very efficient in solving multidimensional problems in a large variety of applications. It has been proposed first by Kennedy and Eberhart [25] for non-linear functions optimization and neural network training. Later on, it has been introduced in electromagnetic research for antenna design [26]-[29], and subsequently it has been applied to artificial ground plane for surface wave antennas [30], microstrip antennas [31]-[33], linear and planar array geometry [34]-[35], log-periodic array dipole antennas, aperture antennas and so on.

PSO takes inspiration from the animal kingdom, in particular from the group movement in search of a common objective. The algorithm consists of a swarm randomly initialized inside a predetermined solution space, which represents the set of the admissible solution for the problem. The quality of the solution is measured through a suitable objective function, associated with each position in the solution space. The choice of the objective function is a key point of every PSO procedure, since it must be accurately defined to well describe the requests of the problem. The group of particles moves iteratively inside the solution space, trying to reach the position which represents the optimal solution, corresponding to the minimum value of the objective function. The movement of each individual is based on its own instinct, on the memory of its path and on the iterations with the other individuals. Each particle is described by a vector of variables x, which are the coordinates of the solution space and, at the same time, the parameters to be optimized. In the j-th iteration, the i-th particle is characterized by its position $x_{i,j}$ (19) and velocity $v_{i,j}$ (20). Next position, direction and velocity of the single particle are updated according to its position and velocity at the previous step, the best solution found by the particle in its path (personal best, *p*) and the best solution found by the whole swarm (global best, *g*):

$$x_{i,j} = x_{i,j-1} + v_{i,j}, \quad (19)$$

$$\begin{aligned} v_{i,j} = w\cdot v_{i,j-1} + c_1\cdot r_1\cdot(p_{i,j} - x_{i,j-1}) + \\ +c_2\cdot r_2\cdot(g_{i,j} - x_{i,j-1}) \end{aligned} \quad , \quad (20)$$

w scales the velocity component at the same direction of the previous step (inertia weight), r_1, r_2 are two random numbers between 0.0 and 1.0 which simulate the random component of the swarm behaviour, c_1, c_2 provide a weight between the pull of *g* and *p*: low values allow particles to roam far from target positions before being attracted to, whereas high values provide movements more strongly orientated to target. Eberhart suggested that the best choice for c_1 and c_2 is 2.0 [36] for most of applications. In general, velocity is applied to position updating for a time-step Δt which is set to 1 in this work.

The algorithm main steps (Fig. 4) are:

1. Initialization of swarm position and velocity.
2. Systematic particles movement in the solution space. For each particle:
   a) Fitness evaluation (*g*, *p* update)
   b) Velocity update
   c) Position update (swarm movement).
3. Iteration of point 2 until a stop criterion (convergence or maximum number of iterations) is reached.

The objective function shown in Fig. 4 contains the electromagnetic problem and evaluates the propagation characteristics of the ridge WG, whose parameters are variable to be optimized and thus the PSO particles' coordinates.

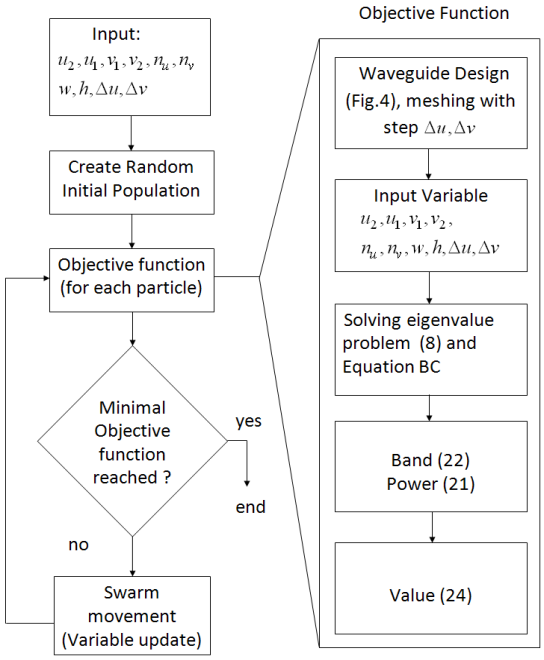

Fig. 4. PSO block diagram.

IV. PARAMETER REW AND SEW

The implementation of an optimization algorithm starts from the definition of the optimization variables, which define the solution space through their constraints. In our case, the variables are the geometrical dimensions of all the ridges (width w and height h) and the horizontal spacing s between them, therefore they constitute the solution space.

The chosen objective function includes both the bandwidth of the simple mode propagation regime, and the maximum power flux. These data can be obtained by the computation of the eigenvalues of the REW (or SEW) section. This is performed by the FDFD described in Section II, after a suitable discretization of the section has been performed. Once the eigenvalue problem is solved we have both the scalar potential and the eigenvalue for the first modes of the guide. From the former, by numerical derivatives, we can compute the mode field [1]. The smallest two eigenvalues k_{TE1}, k_{TE2} gives directly the WG bandwidth. The bandwith is equal to:

$$BW = f_{TE2} - f_{TE1} = \frac{\tilde{c}}{2\pi}\left(k_{TE2} - k_{TE1}\right), \qquad (21)$$

where f_{TE1} and f_{TE2} are respectively, the first and second cut-off frequencies of the TE modes of the SEW and c is the free-space light-speed. The knowledge of the mode distribution allows to compute the power flux P through a transverse section of a SEW or REW using its relationship with the total energy for unit length W_{EM} [4]:

$$P = W_{EM} \cdot \frac{k_z c}{k_0} = \frac{1}{\sqrt{\varepsilon_0 \mu_0}} \cdot \frac{\lambda_0}{\lambda_g} \cdot \frac{\varepsilon_0}{2} \cdot \int_S E^2 dS \,. \qquad (22)$$

The electric field in the integral is computed by the E-field distribution on the transverse section given by the FDFD. This distribution is normalised so that max |E| is equal to the field at the dielectric breakdown (E_{BD}), so (3) actually gives the maximum power.

Then an appropriate objective function is devised to select the best-suited solution for the trade-off request between a large bandwidth (21) and a large power flux (22).To devise the objective function, the ratio between the actual SEW properties and the rectangular WG ones are considered. This is done for bandwidth and high power handling capability (PHC):

$$R_B = \frac{BW_{rect}}{BW_{SEW}} \qquad R_P = \frac{P_{rect}}{P_{SEW}} \quad , \qquad (23)$$

where BW_{rect}, BW_{SEW} and P_{rect}, P_{SEW} are, respectively, the bandwidth, the PHC of R-WG [37] and SEW. The power flux (P) computed from (21) depends on E_{BD} so, as the field distribution in (21) is normalized, R_P is evaluated at the same maximum field in the WG.

The objective functions is:

$$f_p(k) = \left|\frac{R_P}{k} - 1\right| + R_B^2 . \qquad (24)$$

This objective function allows to maximize the PHC with the constraint of bandwidth a k-times reduction in the PHC (24). The configuration has been tested with 20 particles in the swarm, with constant accelerations equal to c1 = c2 = 2. The BW has been optimized with respect to a power reduction by a factor 2 and 3, thus considering $f_p(2)$ and $f_p(3)$.

V. RESULTS

A. FDFD validation

The FDFD for elliptic ridge waveguide described in the previous sections has been extensively validated, to evaluate its accuracy and effectiveness. In the simulations presented in this section we will consider first a sector of elliptic ridged waveguide (see Fig. 5) and then a ridged sector. All dimensions have been normalized to the minor semi-axis of the ellipse.

The FDFD procedure has been assessed against the analytical results of [38]. The resulting eigenvalue problem has been solved using standard MATLAB routines, on a PC with two Intel Xeon E5504 CPUs@2.00 GHz, 48 GB RAM, OS: MS Windows 7 Professional. The results are shown in the next tables. It appears that an FDFD approach provides a very high accuracy: the difference with respect to the analytic accurate data presented in [38] is smaller than 0.02% in most cases.

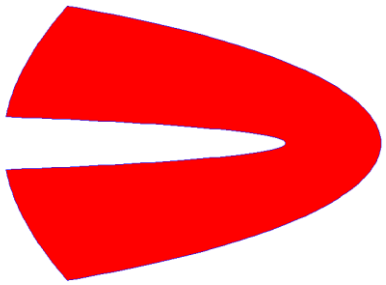

Fig. 5. Elliptic sectoral guide $u \in (u_1, u_2)$, $v \in (v_1, v_2)$, with $u_1 = 0.1$, $u_2 = 0.5$ and $v_1 = -50°$, $v_2 = 50°$.

The total time spent by the FDFD approach is given by the matrix filling time and by the eigenvalue and eigenvectors extraction. For example, for a grid with $\Delta u = 0.0040$, $\Delta v = 0.0009$ and 1010000 points, the filling matrix time is 2,07 sec and the time to extract eigenvalue and eigenvectors is 93.02 sec. The k_t normalized with respect to the focal length, of the first three modes are shown in Table 1.

In Fig. 6, left, we shown the contour plots of the

potential eigenfunctions for the first three TE modes (corresponding to the data of Table 1).

In order to show the flexibility of this approach, a different ridged sector has been considered. Only the eigenfunctions has been reported, since no analytic data are available.

Table 1: Analytical [38] and FDFD k_t, for the guide of Fig. 5. $\Delta u = 0.00563$, $\Delta v = 0.00017$

Modes	$k_t \cdot a$ [38]	$k_t \cdot a$ (our)
1TE	2.6564	2.6564
2TE	6.8370	6.8370
3TE	9.5446	9.5448
1TM	14.2832	14.2831
2TM	14.2995	14.2999
3TM	19.5616	19.5594

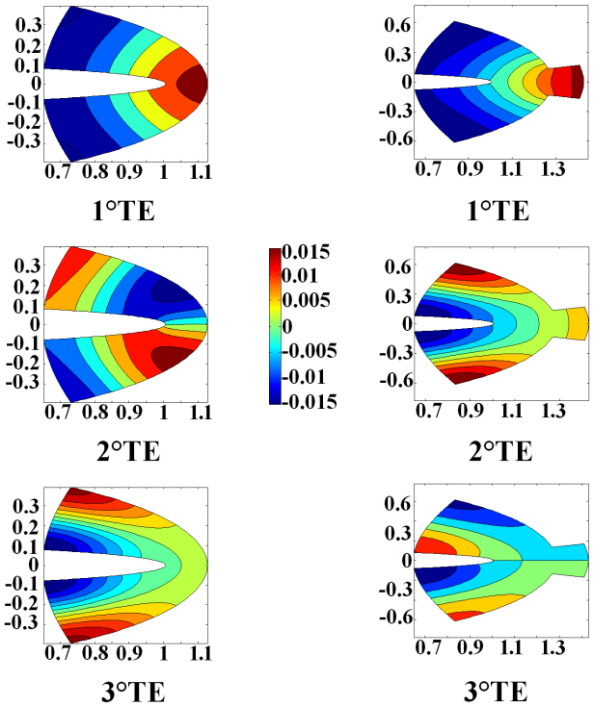

Fig. 6. Lowest-order eigenvectors for the examples presented. (a) Left: structure of Fig. 4. (b) Right: ridged sectoral guide with $u_1 = 0.1$, $u_2 = 0.74$, $v_1 = -50°$, $v_2 = 50°$ and $u_3 = 0.1$, $u_4 = 0.9$, $v_3 = -10°$, $v_4 = 10°$.

B. Constraints and optimal dimensions

The correct scaling of the variables has been obtained by choosing as variables the ratio to the upper ridge part and by imposing the constraints shown in Table 2. In the Table 3 summarize the optimal dimensions and the performance of the considered structure of Fig. 7. The structure SEW (Fig. 7) require six variables in the PSO algorithm.

Table 2: Constraints for staircase SEW

$w_1 = w$	
$w_2 = Aw_1$	A∈[0.01:0.99]
$w_3 = Bw_2$	B∈[0.01:0.99]
$h_1 = Ch_2$	C∈[0.01:0.99]
$h_2 = Dh_3$	D∈[0.01:0.99]
$h_2 = h$	
$6\Delta v h_{u,v} \le w \le (v_2 - v_1) h_{u,v} - 4\Delta v h_{u,v}$	
$4\Delta v h_{u,v} \le w_2$	
$2\Delta v h_{u,v} \le w_3$	
$\Delta u h_{u,v} \le h_1$	
$2\Delta u h_{u,v} \le h_2$	
$3\Delta u h_{u,v} \le h_3 \le (u_2 - u_1) h_{u,v} - 2\Delta u h_{u,v}$	

Table 3: Optimal Dimension of SEW.

Objective Function	$w_1 / h_{u,v}$	$w_2 / h_{u,v}$	$w_3 / h_{u,v}$	
$f_p(2)$	1.19	1.17	1.15	
$f_p(3)$	4.72	1.02	0.99	
Objective Function	$h_1 / h_{u,v}$	$h_2 / h_{u,v}$	$h_3 / h_{u,v}$	*BW* (*GHz*)
$f_p(2)$	0.01	0.02	0.09	3.55
$f_p(3)$	0.01	0.09	0.94	3.86

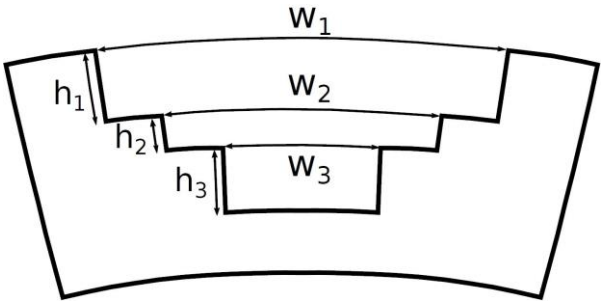

Fig. 7. A typical SEW with $u_1 = 0.1$, $u_2 = 0.5$ and $v_1 = -5°$, $v_2 = +5°$.

VI. CONCLUSION

An approach to the FDFD computation of modes of SEW and REW have been presented. An elliptic mesh has been used in order to avoid staircase approximations of the boundary. The presented results show both the flexibility of the method, as well its simplicity for the computation for TE and TM modes in SEW and REW. Moreover the effectiveness of PSO in the geometrical optimization of a SEW has been illustrated.

ACKNOWLEDGMENT

Marco Simone gratefully acknowledges Sardinia Regional Government for the financial support of his Ph.D. scholarship (P.O.R. Sardegna F.S.E. Operational Programme of the Autonomous Region of Sardinia, European Social Fund 2007-2013 - Axis IV Human Resources, Objective l.3, Line of Activity l.3.1.).

The authors would like to thank George Evers for making freely available its MATLAB PSO Research Toolbox which has been used for simulations.

This work was supported in part by Regione Autonoma della Sardegna under contract CRP-49231 (CUP C45E120000200002).

REFERENCES

[1] R. E. Collin, *Field Theory of Guided Waves*, 2nd ed., New York, IEEE Press, 1991.

[2] J. Helszajn, *Ridge Waveguides and Passive Microwave Components*, London, IEE, 2000.

[3] S. B. Cohn, "Properties of ridged waveguide," *Proceedings of the IRE*, vol. 35, pp. 783-788, August 1947.

[4] S. Hopfer, "The design of ridge waveguide," *IRE Transactions on Microwave Theory and Techniques*, vol. MTT-3, pp. 20-29, October 1955.

[5] R. Sorrentino, *Transverse Resonance Technique*, in Numerical Techniques for Microwave and Millimeter Wave Passive Structures, Chapter 11, New York, John Wiley, 1989.

[6] A. A. El-Sherbiny, "Cutoff wavelengths of ridged, circular, and elliptic guides," *IEEE Transactions on Microwave Theory and Techniques*, MTT-21, pp. 7-12, January 1973.

[7] A. E. Williams and A. E. Atia, "Dual-mode canonical waveguide filters," *IEEE Transactions on Microwave Theory and Techniques*, vol. 25, no. 12, pp. 1021-1026, December 1977.

[8] R. Behe and P. Brachat, "Compact duplexer-polarizer with semicircular waveguide," *IEEE Transactions on Antennas and Propagation*, vol. 39, pp. 1222-1224, August 1991.

[9] B. V. de la Filolie and R. Vahldieck, "Coaxial and circular waveguide band-pass filters using printed metal inserts," *IEEE MTT-S International Microwave Symposium Digest*, pp. 905-908, Albuquerque, New Mexico, June 1992.

[10] J. Huang, R. Vahldieck, and H. Jin, "Computer-aided design of circular ridged waveguide evanescent-mode bandpass filters using the FDTLM method," *IEEE MTT-S International Microwave Symposium Digest*, pp. 459-462, Atlanta, GA, June 1993.

[11] U. Balaji and R. Vahldieck, "Mode matching analysis of circular-ridged waveguide discontinuities," *IEEE Transactions on Microwave Theory and Techniques*, vol. 46, pp. 191-195, February 1998.

[12] L. J. Chu, "Electromagnetic waves in elliptic hollow pipes of metal," *Journal of Applied Physics*, vol. 9, pp. 583-591, September 1938.

[13] N. Marcuvitz, *Waveguide Handbook*, Peregrinius, London, 1986.

[14] J. G. Kretzschmar, "Wave propagation in hollow conducting elliptical waveguides," *IEEE Transactions on Microwave Theory and Techniques*, vol. 18, iss. 9, pp. 547-554, September 1970.

[15] D. L. Young, S. P. Hu, C. W. Chen, C. M. Fan, and K. Murugesan, "Analysis of elliptical waveguides by the method of fundamental solutions", *Microwave and Optical Technology Letters*, vol. 44, pp. 552-558, February 2005.

[16] G. P. Zouros, "Exact cutoff wave numbers of composite elliptical metallic waveguides," *IEEE Transactions on Microwave Theory and Techniques*, vol. 61, iss. 9, pp. 3179-3186, September 2013.

[17] A. Fanti, G. Mazzarella, G. Montisci, and G. A. Casula, "VFD approach to the computation TE and TM modes in elliptic waveguide on TM grid," *Applied Computational Electromagnetics Society (ACES) Journal*, vol. 28, no. 12, pp. 1205-1212, December 2013.

[18] C. S. Lavranos and G. A. Kyriacou, "Eigenvalue analysis of curved waveguides employing FDFD method in orthogonal curvilinear co-ordinates," *IEE Electronics Letters*, vol. 42, no. 12, pp. 702-704, June 2006.

[19] C. S. Lavranos and G. A. Kyriacou, "Eigenvalue analysis of curved waveguides employing an orthogonal curvilinear frequency-domain finite-difference method," *IEEE Transactions on Microwave Theory and Techniques*, vol. 57, iss. 3, pp. 594-611, March 2009.

[20] G. Tsogkas, D. Georgios, J. A. Roumeliotis, and S. P. Savaidis. "Cutoff wavelengths of elliptical metallic waveguides," *IEEE Transactions on Microwave Theory and Techniques*, vol. 57, iss. 10, pp. 2406-2415, October 2009.

[21] A. Fanti, L. Deias, G. A. Casula, and G. Montisci, "A fourth order FDFD approach for the analysis of sectorial elliptic waveguides," *Applied Computational Electromagnetics Society (ACES) Journal*, vol. 30, no. 5, pp. 488-495, May 2015.

[22] A. Fanti and G. Mazzarella, "Curvilinear finite difference approach to the computation of modes of Circular and Elliptic Waveguides," *IEEE Proc. Int. Conf. on Applied Electromagnetics and Communications, (ICECom 2010), Dubrovnik*, Croazia, 20-23 September 2010.

[23] M. N. O. Sadiku, *Numerical Techniques in Electromagnetics*, Boca Raton, CRC Press, 2001.

[24] http://mathworld.wolfram.com/EllipticCylindricalCoordinates.html

[25] J. Kennedy and R. Eberhart, "Particle swarm

optimization," *Proceedings of IEEE International Conference on Neural Networks*, vol. 4, pp. 1942-1948, Perth Wash, Australia, November 1995.

[26] J. Robinson, S. Sinton, and Y. Rahmat-Samii, "Particle swarm, genetic algorithm, and their hybrids: optimization of a profiled corrugated horn antenna," *IEEE Antennas and Propagation Society International Symposium 2002*, vol. 1, pp. 314-317, San Antonio, Texas, June 2002.

[27] J. Robinson and Y. Rahmat-Samii, "Particle swarm optimization in electromagnetics," *IEEE Transactions on Antennas and Propagation*, vol. 52, iss. 2, pp. 397-407, February 2004.

[28] N. Jin and Y. Rahmat-Samii, "Particle swarm optimization for antenna designs in engineering electromagnetics," *Journal of Artificial Evolution and Applications*, vol. 2008, no. 9, 2008.

[29] H. Wu, J. Geng, R. Jin, J. Qiu, W. Liu, J. Chen, and S. Liu, "An improved comprehensive learning particle swarm optimization and its application to the semiautomatic design of antennas," *IEEE Transactions on Antennas and Propagation*, vol. 57, iss. 10, pp. 3018-3028, October 2009.

[30] E. Carrubba, A. Junge, F. Marliani, and A. Monorchio, "Particle swarm optimization for multiple dipole modeling of space equipment," *IEEE Transactions on Magnetics*, vol. 50, iss. 12, pp. 1-10, December 2014.

[31] Y. Choukiker, S. K. Behera, D. Mishra, and R. K. Mishra, "Optimization of dual band microstrip antenna using PSO," *Applied Electromagnetics Conference (AEMC)*, Kolkata, India, pp. 1-4, December 2009.

[32] A. A. Minasian and T. S. Bird, "Particle swarm optimization of microstrip antennas for wireless communication systems," *IEEE Transactions on Antennas and Propagation*, vol. 61, iss. 12, pp. 6214-6217, December 2013.

[33] A. Deb, J. S. Roy, and B. Gupta, "Performance comparison of differential evolution, particle swarm optimization and genetic algorithm in the design of circularly polarized microstrip antennas," *IEEE Transactions on Antennas and Propagation*, vol. 62, iss. 8, pp. 3920-3928, August 2014.

[34] M. M. Khodier and C. G. Christodoulou, "Linear array geometry synthesis with minimum side lobe level and null control using particle swarm optimization," *IEEE Transactions on Antennas and Propagation*, vol. 53, iss. 8, part 2, pp. 2674-2679, August 2005.

[35] D. Cao, A. Modiri, G. Sureka, and K. Kiasaleh, "DSP implementation of the particle swarm and genetic algorithms for real time design of thinned array antennas," *IEEE Antennas Wireless Propagation Letter*, vol. 11, pp. 1170-1173, 2012.

[36] R. C. Eberhart and Y. Shi, "Particle swarm optimization: Development, applications and resources," *Proceedings of the 2001 Congress on Evolutionary Computation*, COEX Seoul, Korea, vol. 1, pp. 81-86, May 2001.

[37] M. Simone, A. Fanti, and G. Mazzarella, "Ridge waveguide optimization with PSO algorithm," *Journal of Electromagnetic Waves and Applications*, vol. 2, iss. 29, pp. 199-209, February 2015.

[38] G. Amendola, G. Di Massa, and G. Angiulli, "Elliptic-hyperbolical waveguides," *Journal of Electromagnetic Waves and Applications*, vol. 14, iss. 11, pp. 1473-1487, 2000.

Alessandro Fanti received the Laurea degree in Electronic Engineering and Ph.D. degree in Electronic Engineering and Computer Science from the University of Cagliari, Cagliari, Italy, in 2006 and 2012, respectively. He urrently holds a post-doc scholarship for design of microwave components. His research activity involves the use of numerical techniques for modes computation of guiding structures, optimization techniques, analysis and design of waveguide slot arrays, analysis and design of patch antennas.

Marco Simone graduated in Electronic Engineering at the University of Cagliari on 2011 and currently is a Ph.D. student in Electronic Engineering and Informatics at University of Cagliari. His research activity involves the use of optimization techniques for microwave devices.

Luisa Deias received the Laurea degree in Electronic Engineering and Ph.D. degree in Electronic Engineering and Computer Science from the University of Cagliari, Cagliari, Italy, in 2002 and 2006, respectively. She worked as Post-doctoral Fellow in the Electro-magnetic Group at the University of Cagliari from 2006 to 2013. Her research interests include numerical techniques in electromagnetism, metamaterial analysis and optimization, microwave components and antennas analysis and design.